Sustainable Earth Review

Geological and petrophysical studies of some soil erosion-prone zones within Okigwe and Umuahia areas, southeastern Nigeria

Hope Onyechigoziri Isreal[a], Alexander Iheanyichukwu Opara[a], Diugo Okereke Ikoro[a], Bridget Odochi Ubechu[a], Kelechi Dennis Opara[a], Henry Nkemakolam Echetama[a], Chinyere Caroline Amadi[a], Timothy Chibuike Anyanwu[a*] [iD]

[a] Department of Geology, Federal University of Technology, Owerri, Imo State, Nigeria

ABSTRACT

Geological and petrophysical studies of some erosion prone soils around Okigwe and Umuahia area, southeastern Nigeria was carried out to determine the erodibility and erosivity characteristics of the study area. Soil samples were collected with a soil auger at a depth range of 0-2m. Analyses carried out include the determination of petrophysical properties (porosity, permeability), and sieve analysis. Grain size analysis revealed sorting coefficients of 0.36-1.32, and graphical kurtosis of 0.51-1.49. The soils are predominantly well to moderately sorted, strongly coarsed skewed and leptokurtic. The sand/sandstone is 87-100% sand with little or no fines with the percentage moisture content ranging from 3.8-26.7%. Estimated permeability values ranges between 0.12-0.46cm/s while the porosity values are between 32.2-37.8%. Result of this study thus revealed that the area is characterized by an interlaying of clay/shale and sandstone units. The accumulation of water at the contact of the shale/sandstones units decreases the shear strength of the sandstone which further reduces the stability and results in the slipping off of the sandstone unit. The slipped sandstone is later carried away by runoff thereby leading to gully development.

1. Introduction

Soil erosion is the systematic removal and transportation of soil particles by the erosive agents of water and wind. Several theories which have tried to explain the development of soil erosion through the primary erosional processes are recorded in some key publications (Egboka and Okpoko, 1984; Casasnovas and Zaragoza, 1996; Simpson, 2001; Carey, 2006; Ustun, 2008; Ismail, 2008; Ibitoye et al., 2008). Soil erosion in southeastern Nigeria are generally associated with several factors which include high rainfall intensity, poor drainage, wind action, slope instability, poor engineering and agricultural practices by earlier scholars (Egboka and Okpoko, 1984; Ofomata, 1988, 1989; Ofomata et al., 2009). However, anthropogenic activities tend to accelerate erosional processes in the study area.

In addition, some endogenic factors which may include the existence of some particular geological and geomorphic features such as weak zones may have serious implications (Onu and Opara, 2010). The study area is underlain by the Imo Shale and Ameki Formations. The Eocene to Oligocene aged Ameki Formation is composed of medium to coarse-grained whitish sandstone, bluish calcareous siltstone, with spotted clays and thin limestone.

The lithological sections are laterally variable. The lower units are made up of fine to coarse-grained sandstone lenses, with dominantly calcareous shales and thinly bedded shaly-limestone. This Formation overlies the Paleocene Imo shale characterized by vertical to lateral lithologic variations (Uma, 1989; Akpabio and Ekpo, 2008).

The Ameki Formation overlies the Imo Formation vertical, but the stratigraphic boundaries between the Ameki Formation and the Imo Formation have not been precisely defined. Lithostratigraphic sections in the Ameki Formation are described using two different groups: an upper grey-green sandstones and sandyclay; and a lower unit with fine to coarse sandstones and intercalations of calcareous shale and thinly bedded shelly limestones (Reyment, 1965; Whiteman, 1982; Arua, 1986). The incidence of high porosity and permeability in addition to the loose, friable and uncompacted nature of the Ameki formation makes the area vulnerable to erosion initiation and development (Ofomata, 1989; Ananaba et al., 1991; Onu et al., 1992; Okeke and Agbasoga, 2001; Okeke et al., 2011; Ibe et al., 2000). Gully erosion is a crucial component of land degradation and desertification, which represent a serious danger to the ecosystem and environment (Onu et al., 1992; Vanmaercke et al., 2011). Gullies are described as erosional channels that are deeper than 0.5 meters and are typically brought on by concentrated water flow during and soon after a period of intense rainfall (Ogbukagu, 1988; Akamigbo, 1988; Ofomata, 1989). Gullies typically have a dynamic nature and are influenced by the terrain, soil characteristics, vegetation, climate, and land use. Land cover and land use patterns are spatio-temporal, although topography and soil characteristics are essentially fixed over time. The anthropogenic impacts are typically the main driver of gully erosion potentials, other erosion-prone qualities such as erodible soils, soft uncompacted subsoil, or unstable slopes do exist (Castillo and Gómez, 2016). In order to assess the likelihood of gully initiation and propagation in a particular region of interest, it is crucial for sustainable land use management to have a good understanding of the dynamics of gully erosion, particularly with regard to climate change and land use dynamics (Poesen et al., 2003). In general, gully erosion is frequently linked to changes in catchment hydrology, such as the removal of native vegetation and soil disturbance, and is frequently associated with land degradation brought on by anthropogenic activity (Oygarden, 2003). Gully characteristics and erosion rates have been extensively studied in agricultural settings, but metropolitan areas are also known to experience high rates of erosion, particularly during engineering construction

(Wolman, 1967). Few researches have examined gully erosion in urban contexts (Castillo and Gómez, 2016). Other studies detail the headcut retreat and growth of permanent urban gullies. From 1994 to 2000, Archibold et al. (2003) examined two urban gullies and recorded gully headcut retreat, widening, and deepening. They made the same conclusion about gully erosion made by Guerra and Hoffman (2006) in Brazil and Imwangana et al. (2014) in the Congo. They attributed it to changes in land use. A substantial correlation between soil texture and land usage was discovered by Adediji et al. (2013) when they studied the association between urban land surface characteristics and gully erosion in Nigeria. Recent environmental catastrophes that have significantly altered the terrain in Southeast Nigeria include the formation and spread of erosion gullies (Okpala, 1990; Adekalu et al., 2007). This area is rapidly turning into a badland, with a deformed topography and limited land resources that are being lost to erosion every year. Since erosion has ruined many farmlands and decreased agricultural production, large portions of agricultural lands are becoming unfit for agriculture (Egboka et al., 1990). The elements that cause erosion and the creation of gullies are erosivity and erodibility. Erodibility, in contrast to erosivity, is a function of soil characteristics, topography, and land use management. Erosivity, however, is a function of rainfall, a natural occurrence that is beyond human control and modification. In Southeastern Nigeria, rainfall intensities are typically high, averaging between 100 and 125 mm/h (Obi and Salako, 1995). According to Hudson (1981), rainstorms with an intensity of 25 mm/h or above are typically erosive. Gully erosion often causes major soil losses and produce large volumes of sediment which most often silt up local streams. Earlier scholars have variably linked soil erosion in southeast Nigeria to heavy rainfall, drainage, wind, slope instability, inadequate engineering, and agricultural practices (Egboka and Okpoko, 1984). The soil material is typically loosened, detached, and moved from one location to another by flowing water, waves, wind, moving ice, or other geological forces and bank erosion agents. Erosion is typically induced by a set of physical and chemical processes. Although human activities in the studied area tend to speed up erosion processes, it appears that some

exogenic and endogenic geological features make some portions of the region more prone to erosion than other locations (Onu and Opara, 2010). Existence of specific geological and geomorphic units as well as weak zones are a few of these endogenic causes. In order to establish a potential connection between the initiation and propagation of gully erosion and some geological characteristics of the various formations in the study area, some studies have attempted to characterize soils in gully erosion-prone areas in southeastern Nigeria using geophysical data and other non-evasive techniques (Ananaba, 1991; Onu and Opara, 2010; Onu et al., 2012; Onu and Opara, 2012). Attempts have been made to use geographic information system (GIS) and satellite imagery to map gully erosion zones and their associated land use types (Igbokwe et al., 2008; Okereke et al., 2012; Amangabara et al., 2015; Udoka et al., 2015, 2016). However, there is a dearth of studies on the detailed geological, petrophysical and geotechnical characterization of soils within and around the study area to evaluate their susceptibility to soil erosion. A few studies only highlighted the influence of geology on the soils (Egboka et al., 1990; Ogbukagu, 1988; Egboka and Nwankwor, 1985) and possible tectonic influence on gully initiation and development (Ananaba, 1991; Onu and Opara, 2010) across the study area. This study therefore hopes to address these geological factors and illustrate the significance of these factors by carrying out a detailed characterization of one of the most affected litho-stratigraphic units – the Oligocene Ameki Formation. To investigate the factors that generally affect erosivity and erodibility, geological and petrophysical data were used to assess the factors that initiate gullies in the study area. The objective of this study therefore is to characterize the soils of the study area and to infer the effect of soil properties on gully initiation, formation and development in the area.

1.1. Location, Physiography, and Geomorphology of the study area

The study areas lie within the Tertiary sediments of the Anambra basin around Okigwe and Umuahia covering Umuda, Ude, Isingwu, Ugwuaku, Ndiakeme, and environs, Southeastern Nigeria. The area is accessible by many untarred roads and foot-paths that traversed through the area connecting the villages and nearby towns. The roads, both tarred, untarred, and the foot-paths were used as the traverse lines for data collection. The litho-units (Imo Shale and Ameki Formations) of this study are exposed at various locations within the study area. These outcrops formed the basis for the geological data. The relief is a rugged and undulating land of nearly parallel ridges arranged in linear forms and separated from each other by shallow valleys. The ridges are made up mainly of the more resistant sandstones while the valleys are underlain by the weaker and more labile clay, shale and siltstones. The drainage patterns consist mainly of dendritic and radial patterns while the vegetation cover is that of the Tropical Rain Forest. The study area is located within the coordinates defined by latitudes 5^030^1-5^055^1N and longitudes 7^015^1-7^040^1E (Fig. 1). The study area's climate is characterized by erratic temperature changes and persistent precipitation spreading. There is a tropical wet and dry season, with the dry season starting in October and ending in March, and the rainy season starting in March and ending in October. The longest daylight hours, including November and December, are mostly experienced from January to April. At this time of year, there is an average of six hours of sunlight per day, compared to three hours during the rainy months of May through October. The region's diurnal temperatures range from 18^0C to 34^0C, while the daily mean lowest and maximum temperatures are situated between 19^0C and 28^0C, respectively (Akinsanola and Ogunjobi, 2014). The estimated evapotranspiration rate falls between 1450 and 1460 millimeters per year. Similar to this, there is typically low relative humidity during the dry months of January through March and November through December, when the greatest figure of 95% is recorded. The rainy season, which lasts from April to October, has an average relative humidity value of 97%. (Iwuchukwu et al., 2018). Heavy rains typically fall between July and August, following the migration of Atlantic Ocean marine air to the north. Rainfall and sunny periods alternate due to the strong downpour's set pattern. The start of the rainy season, which lasts through October, is signaled by the month of April. The average annual rainfall ranges from 2500 to 4000 mm, with May through October accounting for 89% of the total (Iwuchukwu et

al., 2018). Regularity and intensity of rainfall in the research area, along with a high rate of surface runoff, cause soil leaching and huge

sheet erosion, which ultimately cause percolation and infiltration into groundwater sources (Ibe et al., 2018).
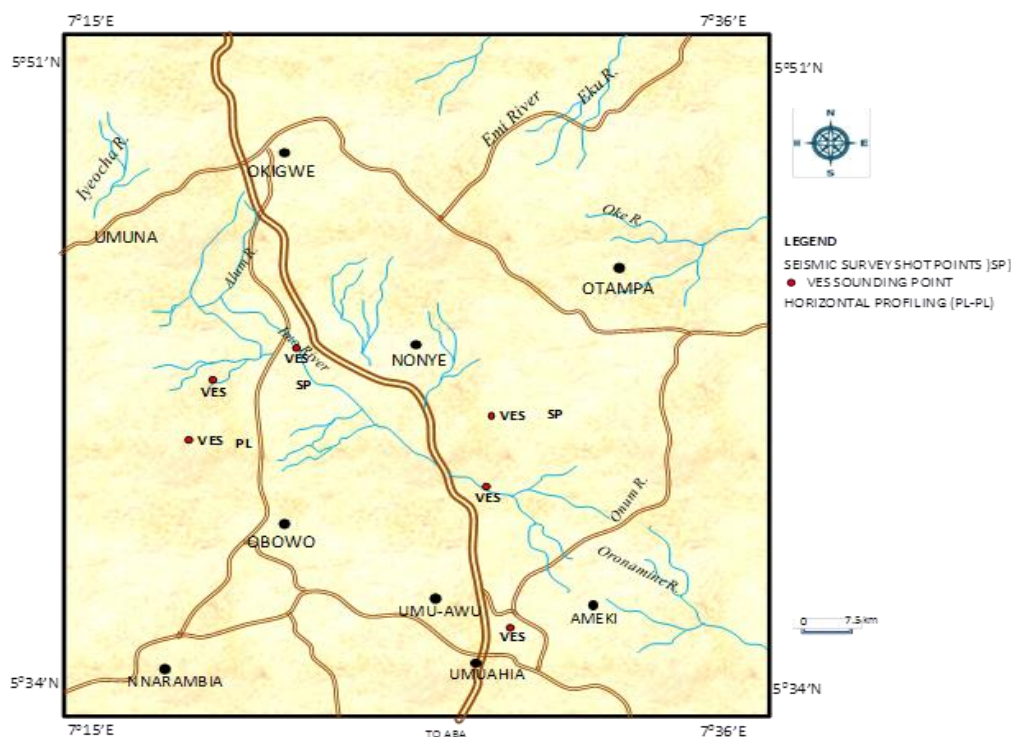

Fig. 1. Location Map of the Study Area showing sampling points

1.2. Geology of the Study Area

The Anambra basin sediments were deposited between the Upper Cretaceous and Tertiary periods. The basin developed after the Santonian tectonism and received its earliest sediment, the Nkporo Group during the Campanian, which consists of transgressive marine Nkporo Shale with its member the Afikpo Sandstone and its lateral equivalent the Enugu Shale containing the Owelli sandstone as a member. The Campanian Nkporo Shale was overlain by the diachronous Campanian-Maastrichtian paralic Mamu Formation- a coal measure formerly known as the Lower Coal Measure. The Mamu Formation is overlain by the continental Maastrichtian Ajali Sandstone. The Ajali Sandstone is overlain by the paralic diachronous Upper Maastrichtian-Danian (Paleocene) Nsukka Formation formerly known as the Upper coal measure. The Nsukka Formation terminated the Upper Cretaceous sediments of the Anambra Basin. The Tertiary sediments of the Anambra basin began with the deposition of the Imo Shale in Paleocene. This formation has its subsurface equivalent to the Akata Formation which was deposited in the

newly developed Niger delta basin. The Imo Shale underlies the younger Eocene Ameki-Nanka Formation. The Ameki-Nanka was in turn overlain by the diachronous Oligocene-Miocene Lignitic Ogwashi-Asaba Formation which fills the Anambra Basin. The Ameki-Nanka and the Ogwashi-Asaba are lateral and time equivalents of the subsurface Agbada Formations of the Niger Delta basin (Fig. 2). Benin Formation is a dominantly continental deposit overlays the Agbada Formation of the Niger Delta Basin (Short and Stauble 1967; Ukpong et al. 2018; Anyanwu et al. 2021; Anyanwu et al. 2022).The formations of interest in this study are the two lithostratigraphic units, namely the Imo Shale (Palaeocene) and Ameki Formation (Eocene) as shown in Figure 3.

1.3. Imo Shale

The type locality of the Imo Shale is along the Imo River between Umuahia and Okigwe in southeastern Nigeria. Reyment (1965) reported that the formation is typically developed as a thick clayey shale, about 1000 m in maximum thickness. The Formation is said to rest

conformably on the Nsukka Formation within Owerri area, and on the northwest flank of the Niger delta Complex, the formation rests conformably on the Cretaceous Abeokuta Formation. According to Dessauvagie (1974), the formation is made up primarily of fine-textured, dark grey and bluish-grey shale with sporadic bands of clay ironstone and sandstone, which are more common nearer the top of the unit. The Imo Shale in western Nigeria grades laterally outward into the Ewekoro limestones. The formation is 1600 feet (487.78 meters) thick at the type locality in Eastern Nigeria, but it is probably only 500 feet thick close to the Ewekoro Cement Quarry (152.4 m). The Akata Shale, which in its type area is about 4000ft (1219.2 m) thick, is where the Imo Shale passed down dip (Whiteman, 1982). In wells in the Araromi and Gbekebo regions of western Nigeria, Reyment (1965) reported a thickness of 3200 ft (975.46 m), with the formation thinning to 640 and 570 feet (195.1 and 173.7 m). Dessauvagie (1974) estimated the Imo River's type localty to be 1600 feet (487.7 meters) thick. Reyment (1965) said that the Imo Shale, which was formed in a marine environment, generally exhibits lateral variation into sandstones in the Eastern region. There is a clear distinction between shallow marine clastic facies and deeper marine clastic facies (Whiteman, 1982). Murat (1970) distinguished between shallow and deep clastic marine environments in the Imo Shale Embayment, which is east of the Okitipupa or Ilesha High and extends into the Anambra basin and beyond into the horst and graben area of the Calabar Flank. Whiteman (1982) reported that the Imo Shales are deposits of the Palaeocene Transgressive Phase while Short and Stauble (1967) regarded the Imo Shale as an up-dip equivalent of the subsurface Akata Formation in the Niger Delta. Table 1 shows the stratigraphic succession within the study area.

1.4. Ameki Formation

The Ameki Formation replaces the Imo Shale Formation at the surface on the Benin Flank and in the Anambra Basin, although it is absent along the Calabar Flank and is associated with the Ogwashi-Asaba Formation (Whiteman, 1982). On the Okitipupa Ridge, to the west of the Niger Delta Complex, the Ameki Formation is believed to pinch out (Fig. 2). The best exposures can be found along the Eastern

Railway Line between Miles 73 and 87, close to Ameki Station, which is why Reyment (1965) chose Ameki as the type locality. White, clayey sandstones and grey-green, sandy clays with calcareous concretions make up the Ameki Formation. There are two distinct lithologic units that can be seen in some places: a lower unit that is composed of fine to coarse sandstones and intercalations of calcareous shale thin shelly limestones; and an upper unit that is made up of coarse, cross-bedded sandstones, fine grey-green sandstone, and sandy clay. Sandstones that are interbedded may be up to 320 feet (97.5 meters) thick (Whiteman 1982). Reyment (1965) referred to the "Bende Sandstone member" with the name Bende. Informally speaking, this is a white calcareous sandstone. The Nanka Sand, which is located in the valley between Nanka and Oko, is thought to be a lateral equivalent of the Ameki Formation in the Onitsha Province (Reyment, 1965). In general, the Ameki Formation is mostly shale west of the Niger River, but it transitions into the sandy Ilaro Formation and the lagoon clay of the Oshoshun Formation north of Lagos in western Nigeria. The Ameki Formation is made up of sandstone and limestone modifications and is located east of the Niger. Parts of the subsurface Agbada Formation and the surface Ameki Formation are analogous. The Ameki Formation is most likely essentially similar to the top Sandstone-Shale alternating unit with thin shales and the lower primarily shaly unit of the Agbada - 2 type section, along with the Ogwashi-Asaba Formation (Short and Stauble, 1967; Ukpong and Anyanwu, 2018). The Ameki Formation exhibits noticeable facies alteration. The formation is 4800 feet (1463 meters) thick and is located close to the type locality in Eastern Nigeria. Thought to pinch out across the Okitipupa ridge, the Ameki Formation is much thinner in Western Nigeria than it is in Eastern Nigeria, where it merges laterally with the Oshoshun Formation. It is somewhat identical to the Agbaba Formation in the Niger Delta. The Ameki Formation is only about 300 feet (91.4 meters) thick locally at outcrop level in western Nigeria. Dessauvagie (1974) reported a thickness of roughly 5000 feet, whereas Reyment (1965) reported a thickness of nearly 4600 ft (1402.1 m) (1524 m). The Anambra Basin and the Niger delta Complex contain the shallow marine clastic Ameki Formation, which was deposited during the Eocene

Regression (Whiteman, 1982). Because the Amaki Formation was formed during a prolonged regressive phase, it has been observed that the Amaki Formation grows progressively sandy along the delta rim (Whiteman, 1982). A shallow marine habitat was created, resulting in a significant variance in the sedimentation pattern (Whiteman, 1982). The Ameki Formation is made up of deltaic deposits that were formed as the delta complex expanded across the continental margin and the Anambra Shelf (Onyekuru et al., 2023). The beach was positioned close below Onitsha during the Oligocene period. Although it is unknown whether the Ameki Formation developed in the Cross River area of the delta complex, it is believed that the complex was less developed at the time than the Benue-Niger Complex.
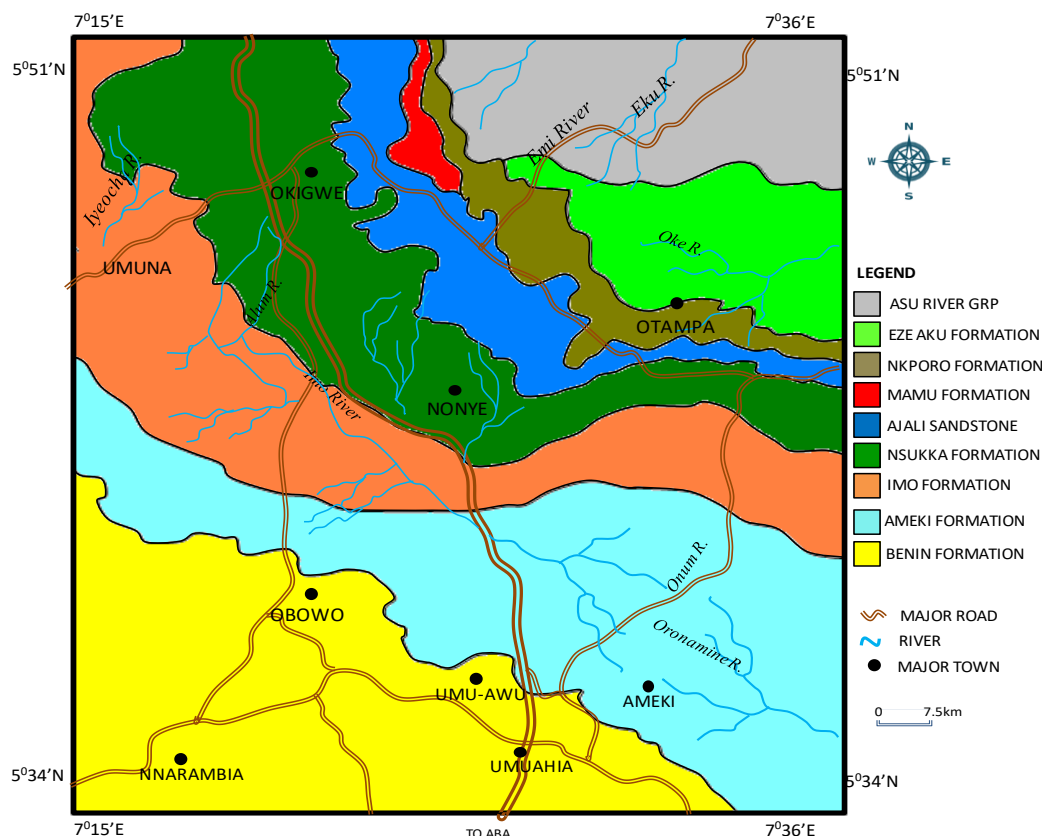

Fig. 2. Geological map of the study area showing the drainages

Table 1. Correlation chart of the Tertiary Niger Delta Succession and Equivalent Outcrops after Reyment (1965).

Age	Surface formation	Subsurface Equivalents	Broad Depositional Environment
Pliocene-recent Miocene – Recent	Coastal Plain Sand Ogwashi – Asaba Formation, Ijebu Formation	Benin Formation Afam and Qua Iboe Clay members	Continental
Eocene – Recent	Ameki Formation Ilaro and Oshoshun Formation	Agbada Formation	Paralic
Paleocene – recent	Imo shale	Akata formation	Marine

2. Material and Methods

2.1. Sample Collection

The samples used for this study were collected within the study area during fieldwork. Samples were collected from the Imo Shale and Ameki Formation outcrops (road cuts along Enugu – Port Harcourt express road) using the soil auger. The samples were collected considering the different identified litho-facies within the road cuts and exposures. On the whole, 25 samples were collected; 16 samples for grain size analysis and 8 samples

for petrophysical analyses. The samples were collected from the units in locations 6, 8 and 10 (Fig. 2). The detailed study of each of the sections of the three locations (Location 6, 8 and 10), as regards stratigraphy, lithology and sedimentary features, contact between the

lithofacies and thickness of each lithofacies was made. All these helped in the interpretation of the sedimentation history (geologic environment of the study area). The breakdown of the samples collected are shown in Table 2.

Table 2. Sampling and sample point description of the study area

Location	Total No. of samples collected	No. of samples for sieve analysis	No. of samples for petrophysical characteristics analysis
6	4	2	2
8	13	9	3
10	8	5	3

The samples were collected from the different sections from the base of the exposure to the top, excluding the laterite (topsoil). Samples for the petrophysical analysis were collected undisturbed (that is without disorganizing the packing system of the grains). This was possible by using the bulk density auger sampler (instrument). The Auger sampler is an instrument that can hold as ring cup of known volume, cross-sectional area and length. During sample collection, a ring cup is fixed to the auger sampler hole and the instrument is fixed to the sample in place and rotated or hit at the head to collect a sample. Samples for sieve analyses were collected under the surface; that is the weathered zones were first removed before collection. The collected samples were labeled in the field for further laboratory analyses. The attitude (orientation) of the beds and some sedimentary structures were measured using a Brunton Compass. Sixteen samples were collected for sieve analysis and eight samples for petrophysical analysis making a total of twenty-four samples. Each of the samples for petrophysical analysis was analyzed for moisture content, bulk density, permeability, and porosity, while each of the other sixteen samples was analyzed for grain size.

2.2. Grain size analysis

All samples for grain size analysis were first oven dried. Samples were sieved according to Folk (1974) and Pettijohn (1975) recommendations. The amount of each sample sieved was 100g. After sieving, the amount of sample by weight retained in each size was determined and recorded. From this record, the percentage weight of each sample retained was calculated and finally, the cumulative frequency percent retained evaluated (Table 3).

A graph of cumulative frequency percent retained versus grain size in Phi/millimeter was plotted on a probability graph paper. Statistical parameters were determined from the curves using Folk (1974) statistical formulae. The phi Value Table and Folk (1974) statistical formulae were therefore used for the calculations.

2.3. Moisture Content Determination

Some fresh quantity of each of the samples for petrophysical analysis was placed in a moisture can of a known weight and its weight determined. The sample and can after weighing were dried in the oven at a temperature of 110^0C for 24 hours. The sample's weight after drying was determined and recorded. By subtracting the weight of the sample after drying from its weight before drying, the weight of moisture lost was therefore determined using equation 1.

$$\frac{Moisture\ loss}{weight\ of\ dry\ samples} \times 100 \qquad (1)$$

2.4. Permeability determination

The permeability test was carried out at the Institute of Erosion Studies, Federal University of Technology, Owerri, Nigeria. The test was carried out with a constant head permeameter instrument. The undisturbed samples collected with the ring cup were first saturated for one day for sand samples, and four days for the clay/shale samples, inside the instrument's saturation basin. After saturation, the permeability test for the samples was performed. In performing the permeability test, several steps were followed. The water contained by the saturated sample still in the basin was run out into a burette. The time taken to run out this water as well as the volume of

water ran out was recorded. The timing was done using a stopwatch while the volume was read from the already graduated burette. The inside and outside height H_1 and H_2 respectively of water for each sample was determined and recorded. Height difference ($H = H_1 - H_2$) was calculated for each sample. The permeability value was then calculated using the formulae

$$K = \frac{QL}{A\,t\,H} \qquad (2)$$

K = Coefficient of permeability (cm/s), Q = Quantity of water discharged during test (cm^3), L = Length between manometer outlet (cm), A = Cross-sectional area of specimen (cm^2) ,t = time required for the quantity of specimen Q to be discharged during the test (s)while H is the head difference in manometer level during the test (cm)

2.5. Porosity determination

Two different methods of porosity determination for the samples (bulk density and saturation methods) are generally used. However, only the bulk density method was used in the present study. With this method, the undisturbed sample collected with the ring cup of known volume, cross-sectional area and length was weighed, and the weight which is equal to the weight of the sample plus ring cup was obtained. The weight of the ring cup was obtained by weighing it empty. The difference between the weight of the sample plus ring cup and the weight of the ring cup gives the weight of the sample alone. Since the volume of the ring cup is known and the sample assumes the value of the ring cup, then the volume of the sample is also known. From these values, the bulk density of each sample was determined using the formular:

$$Bulk\ density = \frac{Total\ mass}{Total\ volume} \qquad (3)$$

Similarly using another relationship, the porosity values were obtained as shown in equation 4.

$$Porosity = \frac{Bulk\ density}{particle\ density} \qquad (4)$$

3. Results and discussion

3.1. Lithological Interpretation

Sample lithologic log of some of the observed outcrops are shown in Figures 3a & b. The logs show a representation of facies in the same outcrop and also in other outcrops. The lithofacies are mainly made up of sand and clay units. The sandstone of location 8 seems to be more massive than those of location 6 and 10. However, there was no clay/shale unit in location 8. In general, all the sections are topped by topsoil or mostly laterite.
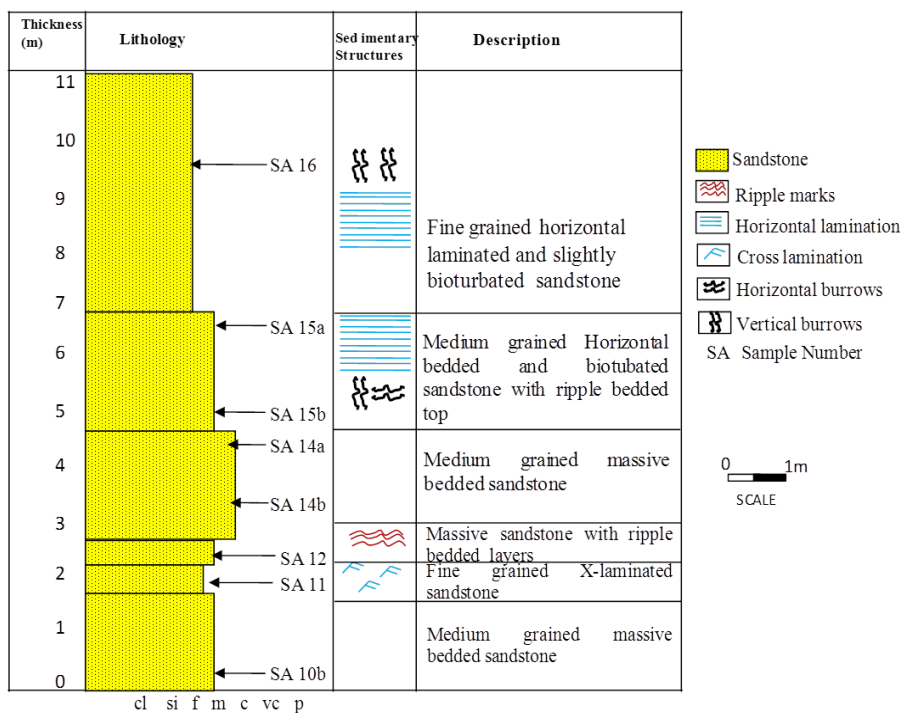
(a)
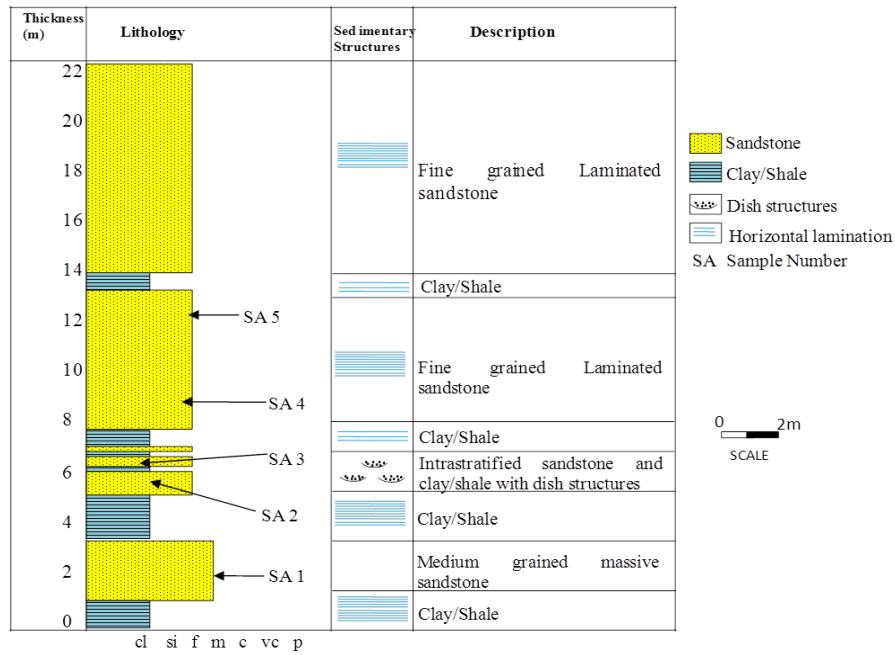
(b)

Fig. 3. Litho-log Section of selected locations in study area: a) Km 132 on Enugu-Port Harcourt Expressway (Imo Shale Formtion), b) Location 10 outcrop at Nkpa-Uboma Junction (Ameki Formation)

3.2. Grain Size Analysis

Grain size analysis was done to obtain the grain size distribution of the clastic particles as they were deposited. The result of the grain size analysis obtained from the study area is shown in Table 3a & b while the grain size distribution curves for the samples are shown in Figs 4a-c. The necessary statistics were obtained using Folk (1974) Statistical formula, and are presented in Tables 3a & b. The verbal classifications were based on the verbal limits of sorting Skewness and Kurtosis according to Folk (1974). Other bases for the verbal classification are the Sediments Triangular Diagram (Folk, 1974) and the Wentworth size class (Folk, 1974). Result of the grain size analysis of the study gave the percentages of mud, sand, and gravel of all the samples collected for the different locations and are presented in Table 4.

(a)

(b)

(c)
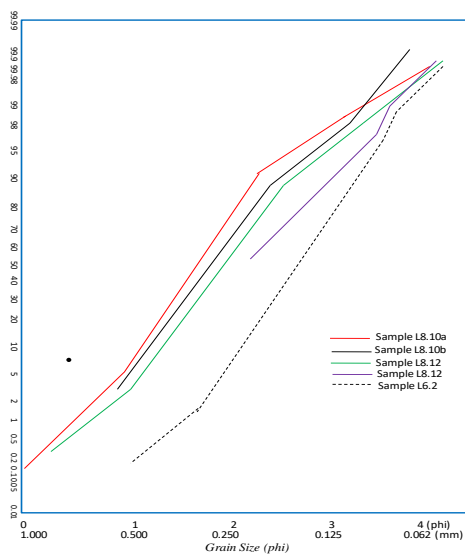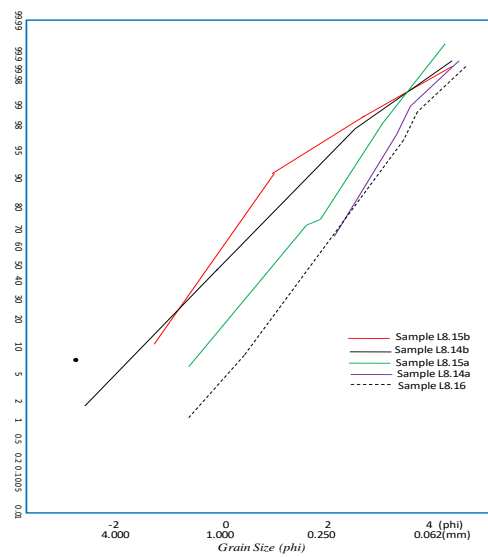
Fig. 4. Some Cumulative Frequency Curves of samples across the study area: a) Locations 6 - 8 samples, b) Samples from Location 8, c) Samples for Location 10

Table 3a. Grain Size Analysis result for Location 6 and 8

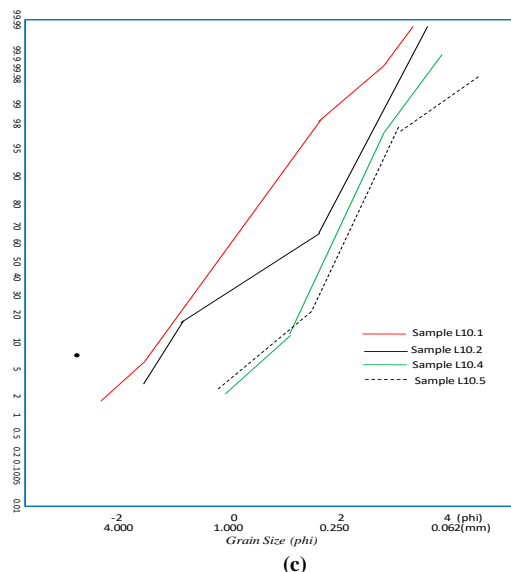| S/N	Sample No.	Median grain size (ϕ)	Graphic mean(ϕ)	Sorting coefficient	Inclusive graphic Skewness	Graphic Kurtosis	Remark
1.	L6.2	2.57(0.17mm)	2.57(0.17mm)	0.36	0.02	1.02	Well sorted sand, near-symmetrical, and mesokurtic
2	L8.10a	1.63 (0.17mm)	1.64(0.32mm)	0.46	0.11	1.19	Well sorted sand, fine skewed, and leptokurtic
3	L8.10b	1.70(0.31mm)	1.75(0.30mm)	0.48	0.73	1.49	Well sorted sand, strongly fine – skewed, and leptokurtic
4	L8.11	2.12(0.73mm)	1.62(0.33mm)	1.16	-0.45	0.50	Poorly sorted sand, strongly coarse skewed, and very platykurtic
5	L8.12	1.79(0.29mm)	1.83(0.28mm)	0.50	0.15	1.14	Moderately well-sorted, sand, fine-skewed and leptokurtic
6	L8.14a	0.73(0.60mm)	0.68(1.62mm)	0.92	-0.10	0.81	Moderately sorted sand, coarse-skewed and platykurtic
7	L8.14b	1.88(0.27mm)	1.92(0.26mm)	0.56	0.10	1.11	Moderately well-sorted sand, near-symmetrical and leptokurtic
8	L8.15a	1.28(0.64mm)	1.36(0.66mm)	0.86	0.13	0.88	Moderately well-sorted, fine skewed and platykurtic
9	L8.15b	0.64(0.64mm)	0.61(0.66mm)	0.57	0.11	0.88	Moderately well-sorted, fine skewed and platykurtic
10	L8.16	1.90(0.27mm)	1.46(0.36mm)	1.06	-0.42	0.51	Poorly sorted sand, strongly coarse-skewed, and very platykurtic

Table 3b. Grain Size Analysis result for Location 10

S/N	Sample No.	Median grain size (ϕ)	Graphic mean(ϕ)	Sorting coefficient	Inclusive graphic skewness	Graphic Kurtosis	Remark)
1.	L10.1	2.25(0.21mm)	2.20(0.22mm)	0.57	-0.10	1.21	Moderately well-sorted sand, coarse-skewed and leptokurtic
2	L10.2	1.45(0.37mm)	1.05(0.48mm)	1.32	-0.36	0.55	Poorly sorted sand, strongly coarse-skewed and very platykurtic
3	L10.4	2.15(0.23mm)	2.18(0.22mm)	0.43	0.02	1.15	Well sorted sand, near-symmetrical and leptokurtic
4	L10.5	0.20(0.87mm)	0.13(0.09mm)	0.91	-0.10	0.91	Moderately sorted sand, coarse-skewed and leptokurtic

Table 4. Percentage of Mud, Sand and Gravel/Pebbles in the different samples

Sample No.	% Mud (Silt)	% Sand	Gravel		Remark
			% Granule	% Pebble	
L6.2	0.4	99.6	-	-	Sand
L8.10a	0.3	99.7	-	-	Sand
L8.10b	-	100	-	-	Sand
L8.11	0.3	99.7	-	-	Sand
L8.12	0.3	99.7	-	-	Sand
L8.14a	0.3	94.7	5.0	-	Slightly granular sand
L8.14b	0.3	99.7	-	-	Sand
L8.15a	0.2	99.8	-	-	Sand
L8.15b	0.2	99.8	-	-	Sand
L8.16	-	100	-	-	Sand
L10.1	0.01	99.9	-	-	Sand
L10.2	-	92.6	7.4	-	Granular sand
L10.4	-	92.6	-	-	Sand
L10.5	-	87.0	11.6	1.4	Granular sand

From Table 4, one could see that samples from location 10 have little or no mud, while samples from locations 6 and 8 have a high percentage of sand, similar to location 10 but contain some

percentage of mud with no gravel. Samples L8.14a, L10.4, and L10.5 contain some amount of gravel. All the samples are sand with little or no mud and gravel. Four samples (L6.2, L8.10a, L8.10b, and L10.4) are moderately well sorted. Three samples (L8.14a, L8.15a, and L10.5) are moderately sorted, while three samples (L8.11, L8.1b, and L10.2) are poorly sorted. Only one sample L8.10b is strongly fine skewed. Four samples (L8.10a, L8.12, L8.15a, and L8.15b) are fine-skewed while three other samples (L6.2, L8.14b, and L10.4) are near symmetrical). Three samples (L8.14a, L10.1, and L10.5) are coarse skewed while three samples (L8.11, L8.16, and L10.2) are strongly coarse skewed. Three samples (L8.11, L8.16, and L.10.2) are very platykurtic, three samples (L8.14a, L8.15a andL8.15b) are platykurtic while only two samples (L6.2 and L10.5) are mesokurtic. However, the rest six samples (L8.10, L8.12, L8.14b, L10.1, and L10.4) are leptokurtic (Table 3).

3.3. Moisture Content

The moisture content of a sample is a function of its pore volume that is occupied by moisture; that is the amount of moisture (water) contained by the sediment. Some sediments can contain a high amount of water (e.g clays) while some contain a very low amount of water (e.g. gravels). The moisture content as earlier stated was determined using the relation;

$$\frac{Moisture\ loss}{weight\ of\ dry\ soil} \times 100\% \qquad (5)$$

or

$$\frac{X-Y}{Y-Z}\,100\% \qquad (6)$$

where X = Weight of can + wet soil (gm), Y = Weight of can + dry soil (gm), $X - Y$ = Weight of water along (gm), Z = Weight of the empty can (gm), and $Y - Z$ = Weight of dry soil alone (gm)

Results for the moisture content determinations are shown in table 5 for all samples analyzed. Analysis of the results revealed that samples L6.P7 and L10.P1 have relatively high-water content values of 26.7% and 25.8% respectively. This is so because they are clay/shale samples that have numerous pore spaces. Samples L8.P5 and L10.P2 have the least water content values 3.6% and 3.8% respectively. This is also attributed to their grain size which is coarse and hence makes the samples have few pore spaces which are connected and hence allows the water to pass through rather than being retained. The water content generally is a function of the pore spaces and their interconnectedness (Porosity and permeability). The water content also depends on the season of collection of the sample. Samples collected during the rainy season have higher water content than samples collected during the dry season. At certain periods during the dry season, samples have very negligible to almost zero water content. The samples for this study were collected in the month of June (rainy season).

Table 5. Water Content of the samples collected from the study area

S/N	Sample No.	Wt of Can(g) [Z]	Wt of Can + Wet [X]	Wt of Can + Dry [Y]	Wt of Water lost (g) [X-Y]	Wt of Dry Sample [Y-Z]	Moisture content (%) [X-Y x 100- Y − Z]
1.	L6.P7	27.2	31.0	30.2	0.8	3.0	26.7
2.	L6.P10	94.9	269.8	250.5	19.3	155.6	12.4
3.	L8.P4	27.7	48.7	47.8	0.9	20.1	4.5
4.	L8.P5	28.0	45.5	44.9	0.6	16.9	3.6
5.	L8.(6	27.3	45.5	44.8	0.7	17.5	4.0
6.	L10.P1	27.6	35.9	34.2	1.7	6.6	25.8
7.	L10.P2	94.8	274.5	268.0	6.5	173.2	3.8

3.4. Permeability

Permeability is a measure of the ease with which fluids can flow through a medium. A sediment is said to be permeable if it allows or permits an appreciable quantity of fluids to pass through it in a given time. This occurs when the sediment contains a reasonable number of pore spaces that are interconnected to each other. From the result of the permeability, the percolation rate, infiltration and runoff rates can

be determined. The coefficient of permeability was determined using a modified version of Darcy's law,

$$q = k\,I\,A \qquad (7)$$

In the experimental procedure described above, the value of I, the gradient was replaced by H/L, where it is the head difference and L is the length between manometer outlets. Additionally, the value of q, the rate of water flow was replaced by Q/t, where Q is the

quantity (in volume) of water discharged, and t is the time required for the quantity to be discharged. Making these substitutions in the equation 7, another equation was thus obtained:

$$K = \frac{\emptyset L}{At\,H} \qquad (8)$$

Where $K =$ Coefficient of permeability (cm/s), $Q =$ Quantity (in volume) of water discharged during test (cm^3), $L =$ Length between manometer outlets (cm), $A =$ Cross-sectional area of specimen (cm^2), $t =$ Time required for quantity Q to be discharged during test (sec) and $H =$ Head difference in manometer level during test (cm). The values of L and A remained constant for all samples and was taken as 5cm and 19.63cm^2 respectively. This is so because the ring cups are equal in volume for all measured samples. Permeability values for all

the samples are shown in table 6. The result shows that two samples (L6.P7 and L10.P1) have no permeability value. These two samples are clay/shale samples; the absence of permeability in the samples could be attributed to the fact that the numerous pores are not interconnected and are microscopic to sub-microscopic in size as expected from clay/shale samples. Sample L10.P2 has the highest permeability value of 0.46cm/s. This could be due to the pebbly nature of the sample which affords the pores good connection with one another, hence good fluid movement. The other samples have reasonable permeability in line with their sandy nature which gives a fairly good interconnection of pores since few fines could otherwise block the connections.

Table 6. Result of the Permeability test of the samples collected from the study area

S/N	Sample	Inside height (H1) in cm	Outside height (H2) in cm	Height difference (H) H=H$_1$ − H$_2$	Quantity of water discharged (Q) in cm^3	Time permeability Discharge of Q (t) in sec	(K) in cm/s K = QL/A t H
1	L6.P7	-	-	-	-	27	-
2	L6.P10	6.5	3.7	2.8	35.3	27.8	0.12
3	L8.P4	6.1	3.7	2.4	28.4	18.8	0.22
4	L8.P5	5.8	3.9	1.9	38.3	19.9	0.26
5	L8.P6	6.1	3.9	2.2	41.5	23.7	0.20
6	L10.P1	-	-	-	-	-	-
7	L10.P2	5.0	3.8	1.2	42.5	19.8	0.46

3.5. Porosity

Porosity is the fraction of the total volume of the sample that is occupied by pore spaces. It is usually expressed as a percentage. Total porosity is the total pore spaces including the interstices and voids whether connected or unconnected. Whereas effective porosity is a measure of the pore space that is connected and can allow the free movement of fluids. Normally total porosity is greater than effective porosity. The bulk density method of porosity determination was adopted using the following formulae:

$$Porosity = 1 - \frac{e\,b}{e\,s} \qquad (9)$$

$$\text{where} \quad eb = \frac{Mt}{Vt} \qquad (10)$$

$eb =$ Bulk density (gm/cm^3) and $e\,s =$ Particle density (Particle density for samples of the study area has an average value of 2.70gm/cm^3.

This value was used for $e\,s$ in this study and was assumed constant for all samples); $Mt =$ Total mass (g) and $Vt = \frac{7}{8}$ Total volume (cm^3). The method depends solely on the density of the sediments. Coarse textured sediments generally have higher particle density than fine texture sediments, thus giving low porosity for coarse grains, and high porosity for fine grains (Babalola, 1988). The porosity values obtained using this method for all samples are presented in Table 7. All the samples show almost similar porosity within the range of 32.2% - 37.8%. Porosity depends mainly on the packing system which somehow depends on the grain size. Poorly sorted samples have low porosity as the finer samples will occupy the spaces created by the bigger ones. Well sorted samples, on the other hand, will have high porosity values.

Table 7. Result of the Porosity test of the samples collected from the study area

S/N	Sample No.	Weight of Ring (g)	Weight of Ring + Sample (g)	Weight of sample (m) in g	The volume of sample (V) in cm^3	Bulk density g/cm^3	Porosity (%) $\frac{-eb}{es}$	$1 - \frac{eb}{es}$

1	L6.P7	96.1	275.6	179.5	98.174	01.83	0.678	32.2
2	L6.P10	94.9	269.8	174.9	98.174	1.78	0.659	34.1
3	L8.P4	87.3	257.9	170.6	98.174	1.74	0.655	35.6
4	L8.P5	95.7	260.5	164.8	98.174	1.68	0.622	37.8
5	L8.P6	96.0	263.2	167.2	98.174	1.70	0.630	37.0
6	L10.P1	98.2	277.5	179.3	98.174	1.83	0.678	32.2
7	L10.P2	94.8	274.5	179.7	98.174	1.83	0.678	32.2

3.6. Discussion

Porosity results from all locations show that the study area has high porosity. The porosity of samples from Imo Shale are slightly higher than those of Ameki Formation (Table 7). The results also show a general high permeability for the area, with the sand unit from location 10 (Ameki Formation), showing the highest permeability (Table 6). The clay from both locations 6 and 10 that is both Imo Shale and Ameki Formation showed no reasonable permeability at all. Hence, they are said to be impermeable from the test (Table 6). The study area showed high water content for the clay/shale but a moderate water content value for the sand sample (Table 5). The grain size result showed variations in both the sorting, skewness and kurtosis nature. The size classes of the sand samples also differed (Tables 3a & b). The high permeability observed in the sandstone samples could be attributed to their very low shale content coupled with the shape of the grain which are not generally uniform. The grains were subangular, subrounded, rounded, etc. This is in agreement with the work of Davis and Dewiest (1966) that "a high angular to subangular particle forms high porosity and permeability sediments due to their corners creating high pore sizes". Small quantity or lack of mud which serves as cementing material results in loose packing and lack of compaction of the particles. This also leads to the presence of more pores that are well connected giving high porosity and permeability. Infiltration is the process of water entry into the immediate soil surface and subsequent movement vertically downwards (Babalola, 1988). It ceases immediately the pores are filled with water or any other material. Thus, if the rate at which water is supplied to the ground especially during a rainstorm or intensive rainfall exceeds the rate at which it can percolate into the ground, the volume that infiltrates will gradually diminish or even become zero (for instance, during consecutive rainy days without sunshine). The movement of water downward into the sediment is known as seepage. Tow forces of attraction are between water molecules and soil particles. Coarse-grained sediments have a high seepage rate while fine-grained sediments have a low seepage rate, just like permeability. This could account partly for why sandstone members of the Imo Shale have little or no water on its surface (waterlogged), while the shale member is mostly logged by water. According to Babalola (1988), sediment texture and structure influence infiltration and thus seepage. When sediment has high porosity, it implies that the void volume of the sediment will be high. Permeability of this same sediment could be high or low pending on some factors such as the sorting or the grains, grain size present, etc. The type of sorting the grains have determines how connected the pores will be and permeability is a function of the pore connections. When the sorting is poor, the fines will occupy part of the void created by the coarse grains and this will somehow reduce the permeability. But when the sorting is well and the grain size if coarse will have more void spaces which will be more connected since there is little or no fines and thus increasing permeability. When the sediment is well sorted and the grain size is more on the fine side, that is the size class of muddy sediment (<0.625), the pore spaces will be less connected thus reducing interconnection. These conditions were observed in some samples of the sample of the study area. Conditions that lead to low permeability (presence of fines) in turn usually leads to low infiltration and seepage. Sandstone samples that showed high porosity, permeability, and low water content will have high infiltration and seepage rate. The sandstone samples in all locations showed high porosity and permeability and thus will have high filtration and seepage, while the clay/shale samples even though they show high porosity had negligible permeability values and hence will show very low infiltration and seepage rate. Similarly, on the other hand, shear strength is a measure of the cohesion of the material in a soil (Lambe et al., 1969). In saturated sediments, two parameters make up the total stress. The

parameters are pore water pressure and effective stress. Pore water pressure is pressure due to the water that occupies the pores in the sediment. Effective stress according to Peck *et al.* (1974), is the excess stress over the neutral stress and acts exclusively between points of contact of the solid constituents. Pore water pressure acts in all directions in the water and solid in equal intensities (Lambe et al., 1969; Terzaghi and Peck, 1976). When pore water pressure is high as a result of high hydrostatic pressure, the shear strength is reduced. This is what happens in the clay/shale units of the sections observed in the study area. This is a result of the accumulation of more water in pores since permeability is low. Their high water content therefore confirmed this. The sandstones had equally low shear strength. This is due to their low fine content which results in weak binding of the sediments. These findings are in line with previous studies around the study area (Jeje and Agu, 1982; Egboka and Nwankwor, 1985; Nwankwor et al., 1998).

4. Conclusion

Most part of the study area is underlain by shale that is less permeable. Seepage and surface runoff from the sandstone supplies the initial forces. During rains, infiltration and seepage will generally be high in the sandstone layer but at the shale/sandstone interface, there will be entrapment of water as a result of the difference in porosity and permeability. High water content usually results to increased pore pressure and complemented by the appreciable drop in gradient (of about 13^0), thus the shale layer acts as a slip plane, causing quicker runoff with slipping and slumping along the sandstone/shale interface. These slipping, sliding and slumping actions of sediments are mechanisms that cause high expansion in the study area.

After careful evaluation of both geological and geotechnical data obtained from the study area, the following recommendations were made.

1. Massive afforestation program must be pursued on sloppy grounds around gully heads, gully slopes and floors. This will provide a sort of canopy to reduce the raindrop velocity and hence the erosivity. Also, the roots of trees can penetrate deeply into the sediments especially the sandy sediments thereby forming an interlocking network capable of binding the sediment together hence increasing their shear strength and also making them more resistant to erosion.

2. Grazing and other erosion aiding activities should be discouraged to help reclaim the land.

3. Grouting can be gainfully employed in the vicinity of the gullies especially on the sandy sediments to form stronger sediment bonds hence decreasing permeability.

4. Impermeable clay/shale zones should be scraped off during construction, additives can also be added to improve the clay/shale permeability before road constructions in the area. This will reduce road failures in the study area.

5. If possible, drainage should be avoided by not interfering with natural drainage during road construction and other infrastructural works.

References

Adediji, A., Jeje, L.K. & Ibitoye. M.O., 2013. Urban development and informal drainage patterns: Gully dynamics in Southwestern Nigeria. *Applied Geography*, 40, 90-102. DOI: 10.1016/j.apgeog.2013.01.012.

Adegoke, O.S., 1969. Eocene Stratigraphy of Southern Nigeria. Bull. Bur. Rech. Geol.Min.

Adekalu, K.O., Olorunfemi, J.A. & Osunbitan, J.A., 2007. Grass mulching effect on infiltration, surface runoff and soil loss of three agricultural soils in Nigeria. *Bioresource Technology*, 98(4), 912-917.

Akamigbo, F.O.R., 1988. Erosion and Changes in Soil Properties, National Workshop on Ecological Disasters: Soil Erosion. *Federal Ministry of Science and Technology*, 166-169.

Akinsanola, A.A. & Ogunjobi, K.O., 2014. Analysis of Rainfall and Temperature variability over Nigeria, Global Journal of Human-Social Science: B Geography, Geo-Sciences. *Environmental Disaster Management*, 14(3), 1-19.

Akpabio, I. & Ekpo, E., 2008. Geo-electric investigation for groundwater development of Southern part of Nigeria. *Pacific Journal of Science and Technology*, 9(1), 219-226.

Amangabara, G., Njoku, J.D. & Obenade, M., 2015. Applying Satellite Remote Sensing and GIS Tools in the study of Gully Erosion. *Journal of Scientific Research and Reports*, 4(3), 233-264. DOI 9734/JSRR/2015/1275

Ananaba, S.E., 1991. Dam sites and crustal megalineaments in Nigeria. *ITC Journal*, 1, 26-29.

Anyanwu, T.C., Ekpo, B.O. & Oriji, B.A., 2021. Geochemical Characterization of the Coastal and Offshore Niger Delta Crude Oils, Nigeria. *International Journal of Advanced Academic Research*, 7(12), 73-87.

Anyanwu, T.C., Ekpo, B.O. & Oriji, B.A., 2022. Biomarker application in the recognition of the geochemical characteristics of crude oils from the five depobelts of the Niger Delta basin. Nigeria, *Iranian Journal of Earth Science*, 14(1), 1-17. DOI: 10.30495/ijes.2022.1943029.1664

Arua, I., 1986. Paleo-environment of Eocene deposits in the Afikpo syncline, southern Nigeria. *Journal of African of Earth Sciences*, 5, 279-284.

Babalola, O., 1988. Soil properties affecting infiltration, runoff, and erodibility; Proceedings of the national workshop on the ecological disaster, soil erosion. Fed. Min. of Sci and Technology. *Lagos*, 131-153.

Carey, B., 2006. Gully erosion; FACTS Journal, Natural Resources and Water, L81, QNRM05374:1-4.

Casasnovas, J.A.M. & Zaragoza, T.C., 1996. Gully erosion mapping by remote sensing techniques: a case study in Anoiapendes Region (NE Spain); Presentadoen el primer Congreso Europeo Sobre le Control de la Erosia, Sitges(Barcelona), 1-5.

Castillo, C. & Gómez, J.A., 2016. A century of gully erosion research: Urgency, complexity and study approaches. *Earth-Science Reviews*, 160, 300-319. https://doi.org/10.1016/j.earscirev.2016.07.009.

Davies, S.N. & De Wiest, R.J.M., 1966. Hydrogeology, John Wiley & Sons, New York, N.Y. 366.

Dessauvigie, T.H.J., 1974. Geological map of Nigeria, 1.1 million. *Nigeria Jourrnal of Minng Geology*, 9(1&2), 1-18.

Egboka, B.C.E., Nwakwor, G.I. & Orajaka, I.P., 1990. Implications of palæo and neo-tectonics in gully erosion-prone areas of southeastern Nigeria. *Natural Hazards*, 3(219), 220-231.

Egboka, B.C.E. & Nwankwor, G.I., 1985. The hydrogeological and geotechnical parameters as causative agents in the generation of erosion in the rain forest belt of Nigeria. J. Afr. Earth. Sci., 3(4), 417-425.

Egboka, B.C.E. & Okpoko, E.I., 1984. Gully erosion in Agulu-Nanka region of Anambra State Nigeria: Challenges in African Hydrology and Water Resources. *Association of Hydrological Sciences*, 144, 335-347.

Folk, R.L., 1974. Petrology of Sedimentary Rocks, Hemphill Publishing Co. Texas.

Guerra, A.J.T. & Hoffman, H., 2006. Urban gully erosion in Brazil. *Geography Review*, 19(3), 26-29.

Hudson, N.W., 1981. Soil conservation. New York: Cornell University Press.

Ibe, F.C., Opara, A.I. & Ibe, B.O., 2020. Application of pollution risk evaluation models in groundwater systems in the vicinity of automobile scrap markets in Owerri municipal and environs, southeastern Nigeria. *Scientific African*, 8, 1-21 https://doi.org/10.1016/j.sciaf.2020.e00450

Ibe, F.C., Opara, A.I., Ibe, B.O., Adindu, B.C. & Ichu, B.C., 2018. Environmental and Health implications of trace metal concentrations in street dust around some electronic repair workshops in Owerri, Southeastern Nigeria. *Environ. Monit Assess*, 190(696), 1-14.

Ibitoye, M.O., Ekanade, O., Jeje, L.K., Awotoye, O.O. & Eludayin, A.O., 2008. Characterisation of Gully formed in built up areas in southwestern Nigeria. *Journal of Geography and Regional Planning*, 1(9), 164-171.

Igbokwe, J.I., Akinyede, J.O., Dang, B., Alaga, T., Onoa, M.N., Nnodud, V.C. & Anike, L.O., 2008. Mapping and Monitoring of the impact of gully erosion in southeastern Nigeria with satellite remote sensing and geographic information system, The International Archives of the Photogrammetry, Remote Sensing and Spatial Information Sciences. XXXVII (88)

Imwangana, F.M., Dewitte, O., Ntombi, M. & Moeyersons, J., 2014. Topographic and road control of mega-gullies in Kinshasa (DR Congo). *Geomorphology*, 217, 131-139.

Ismail, F., Mohamed, Z. & Mukri, M., 2008. A study on the mechanism of internal erosion resistance to soil slope instability. *EJGE*, 13(A), 1-12.

Iwuchukwu, E.I., Asoegwu, S.N. & Okereke, N.A.A., 2018. Modeling monthly relative humidity of Imo and Enugu states for evapotranspiration estimation. *International Journal of Current Trends in Engineering & Research*, 4(10), 1-8.

Jeje, L.K. & Agu, S.N., 1982. Runoff and soil loss from erosion plots in Ife Area in Southwestern Nigeria. *Geo. Eco. Trop*, 16(3), 161-181.

Lambe, T.W. & Whiteman, R.V., 1968. Soil mechanics S I Version. John Wiley and Sons, Inc. New York. Men., 69, 23-48

Murat, R.C., 1972., Stratigraphy and paleogeography of Cretaceous and Lower Tertiary in Southern Nigeria. In: Dessauvagie TFG, Whiteman AJ (ed) Africa Geology. Ibadan Univ. Press, 256-266.

Nwankwor, G.I., Dike, C.E. & Iwuagwu, C.J., 1998. Piping, Quick conditions and liquefaction as factors of gully erosion, A case study of Okwudor-Amucha Gully complex, Imo state Nigeria. *Journal of Mining and Geology*, 34(2), 225-230.

Nwankwor, G.I., Udoka, U.P., Egboka, B.C. & Opara, A.I., 2015. The Mechanics of Civil – Works Induced Gully Erosion: Applications to Development of Preventive Measures in Southern Eastern Nigeria. *Applied Ecology and Environmental Sciences*, 3(2), 60-65.

Nwaogu, C., Okeke, O.J., Adu, S.A., Edeko, B. & Pechanec, V., 2018. Land Use— Land Cover Change and Soil-Gully Erosion Relationships: A Study of Nanka, South-Eastern Nigeria Using Geo-informatics. In: Ivan et al. (ed) Dynamics in Geoscience, Lecture Notes in Geo-information and Cartography, Springer International Publishing AG 2018 I. DOI 10.1007/978-3-319-61297-3_22.

Obi, M.E. & Salako, F.K., 1995. Rainfall parameters influencing erossivity in southeastern Nigeria. *Catena*, 24(4), 275-287. https://doi.org/10.1016/0341-8162(95)00024-5.

Ofomata, G.E.K., 1988a. Soil erosion characteristics in the forest zone of Southeastern Nigeria, Proc. National workshop on ecological disaster: Soil Erosion. Fed. Min. of Sci. and Tech. *Lagos*, 50-67.

Ofomata, G.E.K., 1988b. The management of soil erosion problems in southeastern Nigeria. Proc. *International symposium on erosion in Southeastern Nigeria*, 3-10.

Ofomata, G.E.K., 2009. Soil Erosion in Nigeria: The Views of a Geomorphologist,

www.nuc.edu.ng/nucsite/File/.../No%207%20Inaugra l%20Lecture.pd. Accessed 5 October, 2020.

Ogbukagu, I.N., 1988. Influence of geology on soil erosion. Proc. National workshop on ecological disaster: Soil Erosion. Fed. Min. of Sci. and Tech. *Lagos*, 123-130.

Okeke, O.C. & Agbasoga, J.C., 2001. Evaluation of Ihiagwa Gravel Deposit as Aggregates for Concrete and Highway Pavements. *Journal of Mining and Geology*, 37(1), 77-84.

Okeke, O.C., Ezeoke, E.I. & Onuoha, B.O., 2011. Geotechnical Evaluation of Some Lateritic Soil Deposits in parts of Anambra Basin Southeastern Nigeria, for road construction. Int. *Journal of Environmental Science*, 7(2), 108-115.

Okereke, C.N., Onu, N.N., Akaolisa, C.Z., Ikoro, D.O., Ibeneme, S.I., Ubechu, B., Chinemelu, E.S. & Amadikwa, L.O., 2012. Mapping Gully Erosion Using Remote Sensing Technique: A Case Study Of Okigwe Area, Southeastern Nigeria. *International Journal of Engineering Research and Applications*, 2(3), 1955-1967.

Okpala, A.O., 1990. Nigerian population growth and its implications for economic development. *Scandinavian Journal of Development Alternatives*, 9(4), 63-77.

Onu, N.N. & Opara, A.I., 2010. Soil erosion in southeastern Nigeria: Implications for man and Environment; Seminar Proceedings, APWEN Seminar on, Imperative Actions for water and agriculture, held at the Federal University of Technology, Owerri, Nigeria, 5th –6th October, 2010, 44-59.

Onu, N.N., Ibe, K.K. & Iwuagwu, C.J., 1992. Excess pore pressure. An erosion promoter in the layered sediments of the Ameki Formation, Southeastern Nigeria Journ. of erosion and Env Degradation, 4(3), 19-30.

Onu, N.N. & Opara, A.I., 2012. Analysis and Characterization of Erosion Gullies using Surface Geophysical Data: A Case Study of Njaba River Gully Erosion, Southeastern Nigeria. *Australian Journal of Basic and Applied Sciences*, 6(4), 122-128.

Onu, N.N. & Opara, A.I., 2012. Delineation of Active Linear Features in a Gully Erosion Zone Using Geophysical Methods: Case study of the Okigwe - Umuahia Erosion Belt, Southeastern Nigeria. *International Journal of Science and Technology*, 2(3), 350-360.

Onyekuru, S.O., Achukwu-Ononye, O.U., Ukpong, A.J., Ofoh, I.J., Ibeneme, S.I. & Anyanwu, T.C., 2023. Stratigraphy and Paleoenvironment(s) of the Late Cretaceous Deposits in Ohafia Area, Afikpo Basin, Southeastern Nigeria. *Journal of African Earth Sciences*,   197,   104713 https://doi.org/10.1016/j.jafrearsci.2022.104713

Oygarden, L., 2003. Rill and gully development during an extreme winter runoff event in Norway. *Catena*, 50, 217-242. DOI:10.1016/S0341-8162(02)00138-8.

Peck, R.B., Hanson, W.E. & Thornburn, TH., 1974. Foundation Engineering. 2nd edn. John Wiley and Sons, New York, NY.

Petti –John, F.J., 1975. Sedimentary rocks. Harper and Row Inc. 3rd edn. New York.

Poesen, J., Nachtergaele, J., Verstraeten, G. & Valetin, C., 2003. Gully Erosion and Environmental Change: Importance and Research Needs. *Catena*, 50(2-4), 91-133. DOI: 10.1016/S0341-8162(02)00143-1

Reyment, R.A., 1965. Aspects of the geology of Nigeria: Ibadan Univ. Press. *Ibadan Nigeria*, 90-145.

Short, K.C. & Stauble, A.J., 1967. Outline of the geology of Niger Delta. *AAPG Bulletin*, 51, 761-779.

Simpson, F., Hudic, P.P., Akpokodge, E.G. & Umenweke, M.O., 2001. Strategic water management, Nigeria, People and Systems for water, sanitation and health, 27th WEDC Conference, Lusaka, Zambia, 2001, 402-404.

Terzaghi, K. & Peck, R.B., 1976. Soil Mechanics in Engineering Practice, 2nd edn. John Wiley and Sons, New York, 729.

Udoka, U.P., Nwankwor, G.I., Ahiarakwem, C.A., Opara, A.I. & Emberga, T.T., 2016. Morphometric Analysis of Sub-watersheds in Oguta and Environs, Southeastern Nigeria using GIS and Remote Sensing data. *Journal of Geosciences and Geomatics*, 4(2), 21-28. DOI:10.12691/jgg-4-2-1.

Udoka, U.P., Opara, A.I., Nwankwor, G.I. & Ebhuoma, O.O., 2015. Mapping Land Use and Land Cover in parts of the Niger Delta for Effective Planning and Administration. *International Journal of Scientific & Engineering Research*, 6(12), 274-281.

Ukpong, A.J. & Anyanwu, T.C., 2018. Late Eocene- Early Oligocene Foraminiferal Biostratigraphy and Paleoenvironment of Sediments from"Bera-24 Well" Niger Delta Basin, Southeastern Nigeria. *European Academic Research*, 6(2), 871-891.

Ukpong, A.J., Anyanwu, T.C., Osung, W.E. & Omoko, E.N., 2018. Sequence Stratigraphic Study of "B-24 Well" Northern Depobelt, Niger Delta, Southeastern Nigeria. *Journal of Applied Geology and Geophysics*, 6(2), 20-28.

Uma,   K.O.,   1989.   An   appraisal   of   the groundwaterresources of the Imo River Basin. *Nigerian Journal of Mining and Geology*, 25(1 &2), 305-315.

Utsun, B., 2008. Soil erosion modeling by using GIS and Remote Sensing: A case study, Ganus Mountain; The International Archieves of the Photogrammetry, Remote Sensing and spatial information Sciences xxxvii B7.

Vanmaercke, M., Poesen, J., Maetens, W., de Vente, J. & Verstraeten, G., 2011. Sediment yield as a desertification risk indicator, Science of The Total Environment,   409(9),   1715-25. DOI: 10.1016/j.scitotenv.2011.01.034.

Whiteman, A., 1982. Nigeria: Its petroleum, geology, resources and potential, Graham and Trotman London.

Wolman, M.G., 1967. A cycle of sedimentation and erosion in urban river channels. Geografiska Annaler A, 49, 385-395.